



# On time dependent MHD nanofluid dynamics due to enlarging sheet with bioconvection and two thermal boundary conditions

Danial Habib<sup>1</sup> · Nadeem Salamat<sup>1</sup> · Sohaib Abdal<sup>2</sup> · Imran Siddique<sup>3</sup> · Mehdi Salimi<sup>4,5</sup> · Ali Ahmadian<sup>6,7</sup>

Received: 16 August 2021 / Accepted: 16 December 2021 / Published online: 23 January 2022  
© The Author(s), under exclusive licence to Springer-Verlag GmbH Germany, part of Springer Nature 2022

## Abstract

The current study pertains to heat and mass transportation of magnetic fluid flow having dilute diffusion of nanoparticles and motile microorganisms over a permeable stretched sheet to examine the influence of thermal radiation and activation energy. Similarity functions are utilized to convert the highly mixed non-linear partial differential equations into higher-order non-linear ordinary differential equations. Five coupled equations are derived to be resolved numerically by employing a computing function Bvp4c, built-in Matlab. Two sets of thermal boundaries prescribed surface temperature (PSF) and prescribed heat flux (PHF) are considered. Basic physical quantities, temperature distribution, concentration, velocity field, and motile micro-organism profiles are observed as influenced by emerging parameters. The microorganisms distribution undergoes decreasing behavior against growing values of bio-convection Lewis number and Peclet number. These results are highly useful in the application of heat-transmitting devices and microbial fuel cells. It is seen that decreasing trend is observed in velocity profile when parameters  $Nr$  and  $Nc$  are uplifted. Also, the motility of the nanofluid decreases when the  $Lb$  parameter is raised. On the other hand, an increase in Peclet number  $Pe$  showed a rising trend in motility profile. Additionally, the implications of Brownian motion, Rayleigh number, Bioconvection Lewis number thermophoresis parameter, Peclet number, and buoyancy ratio parameter are discussed. Moreover, the obtained outcomes are validated as compared to the existing ones as limiting cases. Representative findings for microorganism concentration, skin friction coefficient, temperature gradient, local Sherwood number and density number of motile microorganisms, velocity field, temperature, the volumetric concentration of nanoparticles, are discussed in tabulated and graphical form.

**Keywords** Nanofluid dynamic system · Bio-convection · Magneto-hydrodynamics · Activation energy · Multi-slips · Thermal boundaries

**Mathematics Subject Classification** 00-01 · 99-00

## List of symbols

### Latin symbols

$u, v$  Velocity components (m/s)  
 $x, y$  Cartesian coordinates (m)

$t$  Time (s)  
 $u_w$  Stretching velocity of sheet (m/s)  
 $B$  Magnetic field strength (T)  
 $E_1$  Electric field strength (V/m)  
 $J$  Joule current (A)

✉ Mehdi Salimi  
msalimi@stfx.ca

✉ Ali Ahmadian  
ali.ahmadian@ukm.edu.my

<sup>1</sup> Department of Mathematics, K F University of Engineering and I T. R Y Khan, Rahim Yar Khan, Pakistan

<sup>2</sup> School of Mathematics, Northwest University, Xi'an, China

<sup>3</sup> Department of Mathematics, University of Management and Technology, Lahore, Pakistan

<sup>4</sup> Department of Mathematics and Statistics, St. Francis Xavier University, Antigonish, NS, Canada

<sup>5</sup> Center for Dynamics, Faculty of Mathematics, Technische Universität Dresden, 01062 Dresden, Germany

<sup>6</sup> Institute of IR 4.0, The National University of Malaysia, 43600 Bangi, Selangor, Malaysia

<sup>7</sup> Department of Mathematics, Near East University, Nicosia, TRNC Mersin 10, Turkey

$\phi$	Concentration of nanoparticles
$T$	Temperature of nanoparticles(K)
$N$	Micro-organisms distribution
$g^*$	Gravity(m/s <sup>2</sup> )
$k^*$	Mean absorption co-efficient (1/m)
$k$	Thermal conductivity (W/m.K)
$kr$	Rate of chemical reaction
$r_1$	Velocity slip factor
$r_2$	Concentration slip parameter
$r_3$	Motile slip factor
$(\rho C)_f$	Specific heat (J/K)
$\rho_m$	Molecular density
$D_B$	Brownian diffusion coefficient (m <sup>2</sup> /s)
$D_T$	Thermophoresis diffusion coefficient (m <sup>2</sup> /s)
$D_m$	Diffusivity of microorganisms (m <sup>2</sup> /s)
$T_\infty$	Ambient temperature (K)
$\phi_\infty$	Ambient concentration of nanoparticles
$N_\infty$	Ambient micro-organisms distribution
$\tau$	Heat capacitance ratio
$E_a$	Activation energy (J/mol)
$b$	Chemotaxis constant (m)
$W_c$	Speed of gyrotactic cell (m/s)
$n$	Rotation of micro-organisms (1/s)
$q_w$	Heat transfer rate (W/m <sup>2</sup> )
$R_1$	Velocity slip parameter
$R_2$	Solutal slip factor for concentration
$R_3$	Solutal slip factor for micro-organisms
$N_c$	Rayleigh number
$M$	Magnetic parameter
$N_r$	Buoyancy ratio parameter
$R_d$	Radiation parameter
$Pr$	Prandtl number
$N_b$	Brownian motion parameter
$N_t$	Thermophoresis parameter
$E_1$	Activation energy parameter
$E_a$	Electric field parameter
$Le$	Lewis number
$Lb$	Bio-convection Lewis number
$Pe$	Peclet number
$Ec$	Eckert number
$h$	Suction/injection parameter
$A$	Unsteady parameter

### Greek symbols

$\nu$	kinematic viscosity (m <sup>2</sup> /s)
$\sigma^*$	electrical conductivity(S/m)
$\sigma^{**}$	Stefan-Boltzmann constant (W.m <sup>-2</sup> .K <sup>-4</sup> )
$\rho$	Density (kg/m <sup>3</sup> )
$\gamma$	Chemical reaction
$\omega$	Mixed convection parameter
$\pi$	Component of deformation
$\eta$	Similarity variable
$\theta$	Similarity temperature

$\phi$	Similarity concentration of nanoparticles
$\xi$	Similarity density of micro-organisms
$\delta$	Microorganisms difference parameter

### Subscripts

$p$	Nanoparticles
$w$	On the sheet surface
$\infty$	Ambient

## 1 Introduction

A nanofluid is a material made out of nanometer-sized particles or nanoparticles. These nanoparticles are generally developed from metals, oxides, carbides, or nanotubes, air, ethylene glycol, and oil are common basic liquids. Investigations have been sought to improve the thermal conductivity of fluids. The advancement of nanofluids is because of the notable idea of acquainting HTF strong particles with improved thermal conductivity. Choi and Eastman (1995) pioneered the improved heat transfer rate in technology on base liquids, through the utilization of nanoparticles. Buongiorno (2006) proposed significant progression in heterogeneous diffusion of nano-particles for the improvement of heat transfer. Buongiorno also established possible slipping strategies for thermophoresis and Brownian motion in nanofluids. Alblawi et al. (2019) pursued the Buongiorno method to examine the fluid flow over a stretching sheet, stretched out in all networks. Eid et al. (2020) discussed the performance of the boundary layer stream of Carreau nanofluid over a non-linear surfaces with generation/absorption in a permeable medium. Shah et al. (2020) introduced an article that manages the conveyance of blood and the exchange of thermal by methods for a gold micropolar nanofluid in a penetrable pipeline. He et al. (2020) elaborated the stream and heat transfer of CuO-water nanofluid was tried utilizing single-stage and two-stage (mixed) adaptations of various solids (1–4 percent) tube sizes. Gonçalves et al. (2020) opined that there is a quick need to create arrangements that can assist with overcoming current energy utilization and utilization imperatives. Bazdar et al. (2020) demonstrated that the progression of turbulence and heat transfer within a three-dimensional waved miniature channel. Saqib et al. (2019) pronounced the progression of disulfide dependent on generalized nanofluid ethylene glycol over the vertical isothermal plaque. Nasiri et al. (2019) investigated the compressible smooth molecule hydrodynamics (WCSPH) in the nano-liquid stream and heat transfer along the horizontal ring with Reynolds numbers up to 250 is investigated. Jilte et al. (2019) opined that non-renewable energy source fuelled engine vehicles must occur in a cleaner climate. Mir et al. (2020) observed that

0–6 percent volume fraction of nanoparticles with  $Re = 150$ – $700$  in curved geometry to be dictated by a small volume technique utilizing two-stage water/ag nanofluid stream and heat transfer. Khan et al. (2019) studied various slips from the radiation and chemical response over the stretching layer of the magnetohydrodynamic axisymmetric liquid surge. Punith Gowda et al. (2021a) studied magnetic dipole of nanofluid flow over a stretching sheet along with chemical reaction. Abbasi et al. (2021) elaborated water-based nanofluid with temperature-dependent viscosity. Ramesh et al. (2021) studied slip effects of time-dependent micropolar-based Casson nanofluid. Punith Gowda et al. (2021b) elaborated activation energy and chemical reaction impact of Marangoni driven boundary layer flow of a non-Newtonian nanofluid. Similar work on nanofluid using nano-particles was done by (Ahmad et al. 2021; Yahya et al. 2021; Ahmad et al. 2021)

As per general consideration, the implementation of the activation energy in some engineering advances, for example, compact heat exchangers, metallurgy, casting, liquid metal filtration, nuclear reactor cooling, and fusion control, thermal magnetic flux, and heat transfer mechanism. Alamri et al. (2019) appraised the consequences of heat and mass transfer on the second-grade fluid flow, which is subjected to the relaxation of the time. Ellahi et al. (2019a) presented an unconventional mathematical formulation for the electroosmotic of Poiseuille and Couette nanofluids flow. Ahmed et al. (2019) observed the unsteady flow for heat transfer in carbon nanotubes (CNT's) with viscosity over a shrinking surface. Owing to heated, bi-phase, pressure-driven flow in two slippery walls was discussed by Ellahi et al. (2019b).

Microorganisms are the only cellular sorts that live everywhere, like in animals, humans, and plants. Bio-convection is shaped by the zigzag motion of microorganisms in the fluids. These gyrotactic organisms are much denser than water waving in an upward motion. Applications for mixed convection include biofuels, chemicals, ethanol, amino acid microsensors, biotechnology, and various ecosystems. Specific bio convection mechanisms occur, especially due to the movement of different forms of micro-organisms. Bio-convection exists when moving micro-organisms float upwards, which are even thicker than liquids. When the upper surface of the thin suspension becomes too dense due to mobility, the gradient of density reaches a critical point, gravity is destabilized, and eventually, microorganisms fall for bio-convection. Bhatti and Michaelides (2020) observed the features of thermo-bioconvection nanofluid flow with activation energy over a Riga Plate in the presence of micro-organisms. Srinivasacharya and Sreenath (2020) discussed the bioconvection aspects in squeezing a flow of a couple of stress fluids across a non-vertical channel. Shi et al. (2021) discussed the microorganisms with activation energy effects magneto-cross nanofluid. Hamid et al. (2021) discussed

the bio-convection flow of magneto-Cross nanofluid with gyrotactic microorganisms. Yusuf et al. (2021) studied the magneto-bioconvection flow of Williamson nanofluid with gyrotactic microorganisms using entropy generation.

The effects of radiation on the thermal transfer properties of liquids through extended surfaces are currently being studied by a number of researchers. Many important uses in chemical and industrial radiation technologies are material manufacturing, space exploration, glass production, and open-fire room lighting. The use of radiation from lung treatment in radiation therapy persists today. Almheiri et al. (2020) pointed out in this case we show that the long distance between Hawking and the unit operation specifications is resolved by adding news addles to the gravitational path as defined by von Neumann entropy. Bassett et al. (2020) showed the radiation hydrodynamic equations for the smoothing of the hydrodynamics of the particles are derived from the radiation division and hydrodynamics terms of the operator, including the required material motion conditions and the separation of each sequence of equations in time and space. Gorny et al. (1988) analyzed Earth's satellite thermal (STI) images in the 10.5–11.3  $\mu\text{m}$  spectral range showed that the outgoing radiation flux was stable in both time and space compared to the adjacent blocks in a number of linear settings from the seismically active Middle Asian region (Kopet-Dagh, Talasso-Ferghana, and other failures). Adshad et al. 2020 showed the dark radiation is the curvature in Neff during Big Bang nucleon synthesis contributes to spatial variability with helical and deuterium primordial abundances.

The term “Magneto-hydrodynamic” was introduced by Haanas Alfren in 1942 which is defined as the study of fluids that accommodate electrical properties and magnetic behavior. In the current duration, the interpretation of Magneto nano-fluid has precise apprehension in the range/field of chemistry, medical sciences, physics, engineering, geography, and industries. In numerous aspects of life, abundant researches are done on MHD. The effects of magnetohydrodynamics a non-Newtonian fluid flow using a stretching sheet was discussed by Sarada et al. (2021). Abdal et al. (2020) studied time-dependent MHD mixed convection of micropolar nanofluid over a shrinking/stretching sheet. Abdal et al. (2021a) studies uniqueness of MHD Casson nanofluid flow across an extending cylinder. The porous medium and Stefan blowing effects on MHD flow with active and passive control of nanoparticles over the rotating disk is investigated by Rauf et al. (Rauf et al. 2019a; Mabood et al. 2021; Rauf et al. 2019b). Ali et al. (2021) discussed the phenomena of magnetohydrodynamic mass and heat transport over a stretching sheet. Abdal et al. (2021b) discussed the development of heat transportation over an extendable sheet. Abdal et al. (2015), Ali et al. (2020a), Ali

et al. (2020b), Habib et al. (2021) deliberated the distinct flow features of magneto-hydrodynamic.

Our inspiration from the above submissions was developed to explore time depending magnetohydrodynamics of nanofluids over enlarging sheet with bioconvection and radiative implications. Two different sets of thermal heating process are studied, that is prescribed surface temperature (PST) and prescribed heat flux (PHF). Influence of several physical parameters namely unsteady parameter  $A$ , mixed convection parameter  $\omega$ , bioconvection Rayleigh parameter  $Nc$ , buoyancy ratio parameter  $Nr$ , Reynolds number  $Re$ , Magnetic parameter  $M$ , activation energy parameter  $E$ , Brownian motion parameter  $Nb$ , thermophoresis parameter  $Nt$ , Prandtl number  $Pr$ , Peclet number  $Pe$ , Eckert number  $Ec$ , Lewis number  $Le$ , bioconvection Lewis number  $Lb$ , microorganisms difference parameter  $\delta$ , radiation parameter  $Rd$ ,  $R$  suction and injection if ( $R > 0, R < 0$ ) respectively, chemical reaction  $\gamma$  are analyzed graphically and tabular form in detail.

## 2 Physical model and mathematical formulation

The current description is based on unsteady bioconvection of magneto-hydrodynamics, two-dimensional, incompressible, electrically conducting, nanofluid flow over a stretching sheet with chemical reaction and thermal radiation. The applied electric and magnetic fields have respective strengths  $E_1$  and  $B$ . The velocity components are  $u, v$ . Ohm law is followed by electric and magnetic law  $J = \sigma(E + V * B)$ , here  $J$  is joule current,  $V$  denotes fluid velocity,  $\sigma$  stands for electrical conductivity (see (Habib et al. 2022)). In the presence of a small magnetic Reynolds number, it overcomes the impact of Hall current and induced magnetic field.  $u_w(x, t)$  is presenting velocity of the linearly stretching sheet while

$v_w(x, t)$  denoting velocity of mass transfer, stretching surfaces gives x-axis and y-axis components of the velocity and  $t$  is time.  $T_w, \phi_w$  and  $N_w$  are the temperature, concentration, and motile microorganism of the nanofluid,  $T_\infty, \phi_\infty$  and  $N_\infty$  represents ambient temperature, concentration, and microorganisms respectively, at the surface of the stretching sheet (see Fig. 1). Boundary-layer constitutive equations are simulated using the Buongiorno model (Buongiorno 2006). The governing equations for the given problem are as follows (Abdal et al. 2021c, d; Ali et al. 2019):

### Continuity Equation

$$\partial_x u + \partial_y v = 0, \tag{1}$$

### Velocity Equation

$$\begin{aligned} \partial_t u + u\partial_x u + v\partial_y u = & \nu(\partial_{xx} u + \partial_{yy} u) \\ & - \left(\frac{1}{\rho_f}\right)\partial_x p + \left(\frac{\sigma^*}{\rho_f}\right)(E_1 B - B^2 u) + \left(\frac{1}{\rho_f}\right) \\ & \left( (1 - \phi_f)\rho_f \beta^{**} g^*(T - T_\infty) - (\rho_p - \rho_f)g^*(\phi - \phi_\infty) \right. \\ & \left. - (N - N_\infty)g^*\gamma(\rho_m - \rho_f) \right), \end{aligned} \tag{2}$$

### Temperature Equation

$$\begin{aligned} \partial_t T + u\partial_x T + v\partial_y T = & \left(\frac{k}{(\rho c)_f}\right)(\partial_{xx} T \\ & + \partial_{yy} T) + \left(\frac{\sigma}{(\rho c)_f}\right)(uB - E_1)^2 - \left(\frac{1}{(\rho c)_f}\right)(\partial_y q_r) \\ & + \left(\frac{\mu}{(\rho c)_f}\right)(\partial_x u + \partial_y v)^2 + \tau \left( D_B \left( (\partial_x \phi)(\partial_x T) + (\partial_y \phi)(\partial_y T) \right) \right. \\ & \left. + \left(\frac{D_T}{T_\infty}\right)(\partial_x T)^2 + (\partial_y T)^2 \right), \end{aligned} \tag{3}$$

### Concentration Equation

$$\begin{aligned} \partial_t \phi + u\partial_x \phi + v\partial_y \phi = & D_B(\partial_{xx} \phi + \partial_{yy} \phi) + \left(\frac{D_T}{T_\infty}\right) \\ & (\partial_{xx} T + \partial_{yy} T) - (Kr)^2(\phi - \phi_\infty) \left(\frac{T}{T_\infty}\right)^2 \exp\left(\frac{-E_a}{k_1 T}\right), \end{aligned} \tag{4}$$

### Motile density Equation

$$\partial_t N + u\partial_x N + v\partial_y N + [(\partial_y N)(\partial_{yy} C)] \left(\frac{bW_c}{(C_w - C_\infty)}\right) = D_m(\partial_{yy} N). \tag{5}$$

The suitable form of boundary conditions is express below (Abdal et al. 2021b):

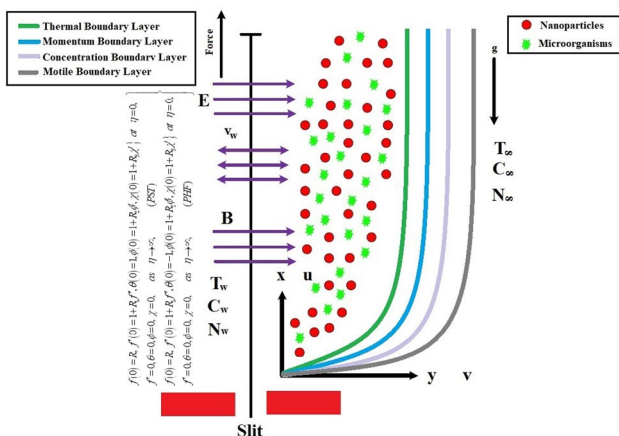


Fig. 1 The schematic flow diagram

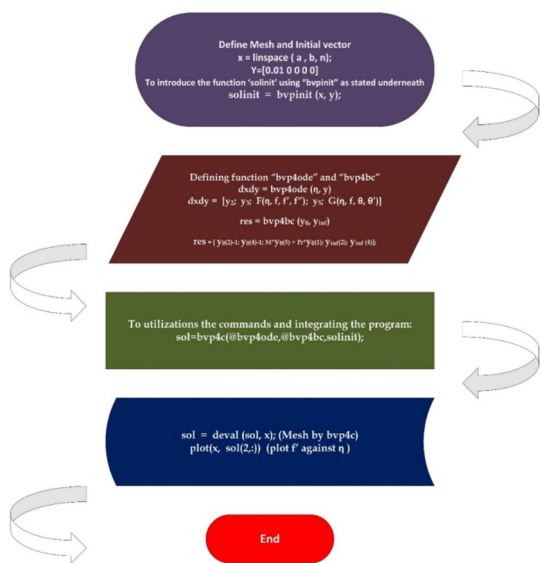


Fig. 2 Flow chart

$$\left. \begin{aligned}
 u &= u_w(x, t) + r_1 \partial_y u, v = v_w(x, t), T = T_w(x, t) = T_c - \frac{cx}{1-at} (PST), \\
 -K \frac{\partial T}{\partial y} &= q_w(x, t) = T_c - \frac{Dx}{1-at} (PHF), \\
 \phi &= \phi_w(x, t) + r_2 \partial_y \phi, N = N_w(x, t) + r_3 \partial_y N \text{ as } y = 0, \\
 u &\rightarrow 0, N \rightarrow 0, T \rightarrow T_c, \phi \rightarrow \phi_\infty, \text{ as } y \rightarrow \infty.
 \end{aligned} \right\} (6)$$

Here,  $r_1 = r_{11} \sqrt{1-at}$ ,  $r_2 = r_{22} \sqrt{1-at}$ ,  $r_3 = r_{33} \sqrt{1-at}$ , signifies the velocity slip factor, concentration slip parameter, motile slip parameter,  $D_B$ ,  $D_T$  and  $D_m$  are the thermophoresis, Brownian motion and microorganisms coefficients,  $\tau = \frac{(\rho c)_p}{(\rho c)_f}$  is heat capacitance ratio,  $k_1 = \frac{k_0}{(1-at)}$  is the heat capacity of the fluid, and  $kr$  is rate of chemical reaction (Fig. 2). Here  $u_w(x, t) = \frac{bx}{(1-at)}$  is velocity of the linear stretching sheet  $v_w(x, t) = \frac{-v_0}{\sqrt{1-at}}$ , is the wall mass transfer, where  $v_w < 0$  denotes injection and  $v_w > 0$  indicates suction.  $\sigma^*$  stand for electric conductivity,  $(\rho c)_f$  indicated the specific heat, component of deformation is  $\pi$ ,  $T_w$ ,  $\phi_w$  and  $N_w$  depicts the temperature of fluid, concentration of nanoparticles and microorganisms concentration at wall, thermal conductivity is  $k_1$ ,  $\phi_\infty$  express the ambient concentration,  $E_a$  is the activation energy. The modified Arrhenius function define as  $(\frac{T}{T_\infty})^2 \exp(\frac{-E_a}{k_1 T})$ ,  $W_c$  show the maximum cell speed of microorganisms and  $N_\infty$  stand for ambient concentration of microorganisms.

The expression for  $q_r$  (Habib et al. 2021),

$$q_r = -\left(\frac{4\sigma^{**}}{3k^*}\right) \partial_y T^4 \tag{7}$$

where  $k^*$  denotes the mean absorption coefficient and  $\sigma^{**}$  is Stefan–Boltzmann constant. Taylor’s series expansion is use for  $T^4$  about  $T_\infty$ . We have (Daniel et al. 2017):

$$T^4 = 4T_\infty^3 - 3T_\infty^4 \tag{8}$$

Then Eq. (7) becomes;

$$\partial_y q_r = -\left(\frac{16T_\infty^3 \sigma^{**}}{3k^*}\right) \partial_{yy} T \tag{9}$$

and Eq. (4) is;

$$\begin{aligned}
 \partial_t T + u \partial_x T + v \partial_y T &= \left(\frac{k}{(\rho c)_f}\right) (\partial_{xx} T + \partial_{yy} T) \\
 &+ \left(\frac{\sigma^*}{(\rho c)_f}\right) (uB - E_l)^2 - \left(\frac{1}{(\rho c)_f}\right) (\partial_y q_r) \\
 &+ \left(\frac{\mu}{(\rho c)_f}\right) (\partial_x u + \partial_y v)^2 + \tau \left(D_B \left((\partial_x \phi)(\partial_x T) + (\partial_y \phi)(\partial_y T)\right)\right. \\
 &\left.+ \left(\frac{D_T}{T_\infty}\right) (\partial_x T)^2 + (\partial_y T)^2\right)
 \end{aligned} \tag{10}$$

Using boundary-layer approximation (Ibrahim and Shankar 2013),

$$\begin{aligned}
 u &\gg v \\
 \partial_y u &\gg \partial_x u, \partial_t v, \partial_x v, \partial_y v \\
 \partial_y p &= 0,
 \end{aligned}$$

the reduced form of Eq. (1) to Eq. (5) are as follows;

$$\partial_x u + \partial_y u = 0 \tag{11}$$

$$\begin{aligned}
 \partial_t u + u \partial_x u + v \partial_y u &= v(\partial_{xx} u + \partial_{yy} u) \\
 &- \left(\frac{1}{\rho_f}\right) \partial_x p + \left(\frac{\sigma^*}{\rho_f}\right) (E_l B - B^2 u) + \left(\frac{1}{\rho_f}\right) \\
 &\left( (1 - \phi_f) \rho_f \beta^{**} g^* (T - T_\infty) - (\rho_p - \rho_f) g^* (\phi - \phi_\infty) \right. \\
 &\left. - (N - N_\infty) g^* \gamma (\rho_m - \rho_f) \right)
 \end{aligned} \tag{12}$$

$$\begin{aligned}
 \partial_t T + u \partial_x T + v \partial_y T &= \left(\frac{k}{(\rho c)_f}\right) (\partial_{yy} T) \\
 &+ \left(\frac{\sigma}{(\rho c)_f}\right) (uB - E_l)^2 + \left(\frac{1}{(\rho c)_f}\right) \left(\frac{16T_\infty^3 \sigma^{**}}{3k^*}\right) \partial_{yy} T \\
 &+ \left(\frac{\mu}{(\rho c)_f}\right) (\partial_x u + \partial_y v)^2 + \tau \left(D_B \left((\partial_x \phi)(\partial_x T) + (\partial_y \phi)(\partial_y T)\right)\right. \\
 &\left.+ \left(\frac{D_T}{T_\infty}\right) (\partial_x T)^2 + (\partial_y T)^2\right)
 \end{aligned} \tag{13}$$

$$\partial_t \phi + u \partial_x \phi + v \partial_y \phi = D_B (\partial_{yy} \phi) + \left( \frac{D_T}{T_\infty} \right) (\partial_{xx} T + \partial_{yy} T) - (Kr)^2 (\phi - \phi_\infty) \left( \frac{T}{T_\infty} \right)^2 \exp \left( \frac{-E_a}{k_1 T} \right) \tag{14}$$

$$\partial_t N + u \partial_x N + v \partial_y N + [(\partial_y N)(\partial_{yy} C)] \left( \frac{bW_c}{(C_w - C_\infty)} \right) = D_m (\partial_{yy} N) \tag{15}$$

The critically investigative assumption of high Reynolds number (Noghrehabadi et al. 2014), The under discussed dimensionless quantities are use to generate the equations (18-21), which are reduced dimensionless form.

$$\eta = \sqrt{\frac{b}{v(1-at)}} y, \quad \psi = \sqrt{\frac{bv}{(1-at)}} x f(\eta), \quad \theta(\eta) = \frac{T - T_\infty}{T_w - T_\infty}, \quad \phi(\eta) = \frac{C - C_\infty}{C_w - C_\infty}, \quad \xi(\eta) = \frac{N - N_\infty}{N_w - N_\infty}, \tag{16}$$

$$T_w(x, t) = T_\infty + T_0 \left( \frac{bx}{2\nu(1-at)^2} \right), \quad \phi_w(x, t) = C_\infty + C_0 \left( \frac{bx}{2\nu(1-at)^2} \right), \quad N_w(x, t) = N_\infty + N_0 \left( \frac{bx}{2\nu(1-at)^2} \right)$$

The stream function can be define as

$$u = \partial_y \psi, \quad u = -\partial_x \psi \tag{17}$$

Utilizing expression (10) then (1-9) becomes

$$f''' - f'^2 - A \left( \frac{\eta}{2} f'' + f' \right) + ff'' + M(E_1 - f') + \omega(\theta - Nr\phi - Nc\xi) = 0 \tag{18}$$

$$\left( 1 + \left( \frac{4}{3} \right) Rd \right) \theta'' + Pr \left( f\theta' - 2f'\theta + Nb\theta'\phi' + Nt\theta'^2 - A \left( \frac{\eta}{2} \theta' + 2\theta \right) + Ec f'^2 + MEc(f' - E_1)^2 \right) = 0 \tag{19}$$

$$f\theta'' + LePr(f\phi' - 2f'\phi - A \left( \frac{\eta}{2} \phi' + 2\phi \right) - \gamma \phi - \sigma(1 + \delta_1 \theta)^n \exp \left( \frac{-E_a}{1 + \delta_1 \theta} \right)) + \left( \frac{Nt}{Nb} \right) \theta'' = 0 \tag{20}$$

$$\xi'' + Lbf\xi' - 2Lbf'\xi - A \left( \frac{\eta}{2} \xi' + 2\xi \right) - Pe[\phi''(\xi + \delta) + \xi'\phi'] = 0 \tag{21}$$

The transform form of boundary conditions (6) are

$$\left. \begin{aligned} f(0) = R, f'(0) = 1 + R_1 f'', \theta(0) = 1(PST),, \\ \theta(0) = -1(PHF), \phi(0) = 1 + R_2 \phi', \xi(0) = 1 + R_3 \xi' \text{ at } \eta = 0, \\ f' = 0, \theta = 0, \phi = 0, \xi = 0 \text{ at } \eta \rightarrow \infty. \end{aligned} \right\} \tag{22}$$

Here  $A(= \frac{a}{b})$  represents the unsteady parameter,  $R_1(= r_1 \sqrt{\frac{b}{v}})$  signify the velocity slip parameter,  $R_2(= r_2 \sqrt{\frac{b}{v}})$  shows the solutal slip factor for concentration and as well as,

$R_3(= r_3 \sqrt{\frac{b}{v}})$  is use for solutal slip parameter for motile microorganisms,  $\omega(= \frac{\beta^{**} g^*(1-\phi_\infty)(T_w - T_\infty)}{u_w b})$  stand for mixed convection parameter,  $Nc(= \frac{\gamma(\rho_m - \rho_f)(N_w - N_\infty)}{\beta^* \rho_f (1-\phi_\infty)(T_w - T_\infty)})$  witnessed the Rayleigh number,  $Nr(= \frac{(\rho_p - \rho_f)(\phi_w - \phi_\infty)}{\beta^* \rho_f (1-\phi_\infty)(T_w - T_\infty)})$  is buoyancy ratio parameter,  $M(= \frac{\sigma^* B_0^2}{b \rho_f})$  is use for magnetic parameter,  $E_1(= \frac{E_a}{KT_\infty})$  is activation energy parameter,  $Nb(= \frac{(\rho c)_p D_B (\phi_w - \phi_\infty)}{v(\rho c)_f T_\infty})$  summarized the Brownian motion parameter,  $Nt(= \frac{(\rho c)_p D_T (T_w - T_\infty)}{v(\rho c)_f T_\infty})$  express the thermophoresis parameter,  $Pr(= \frac{\nu}{\alpha})$  represents the Prandtl number,  $Pe(= \frac{bW_c}{D_m})$

denote the Peclet number,  $Ec(= \frac{u_w^2}{c_p(T_w - T_\infty)})$  signifies the Eckert number,  $E_a(= \frac{E_1}{u_w B})$  is implies the electric field parameter,  $Le(= \frac{\alpha}{D_B})$  is custom for Lewis number,  $Lb(= \frac{\nu_f}{D_m})$  is stand for bioconvection Lewis number,  $\delta(= \frac{N_\infty}{(N_w - N_\infty)})$  is stance for microorganisms difference parameter,  $Rd(= \frac{4\sigma^{**} T_\infty^3}{kk^*})$  is the radiation parameter,  $h(= \frac{v_0}{\sqrt{vb}})$  is use for suction and injection if ( $h > 0, h < 0$ ) respectively,  $\gamma(= \frac{k_0}{b})$  is stance for chemical reaction.

### 3 Physical quantities

The corporal manufacturing quantities of practical interest for engineers are (Abdal et al. 2021b):

#### 3.1 Surface drag force

The skin friction coefficient is defined as

$$C_f = \frac{\tau_w}{\rho u_w^2(x, t)},$$

where,  $\tau_w$  signify shear stress and is defined as

$$\tau_w = \mu(\partial_y u) \text{ at } y = 0,$$

Thus

$$C_f Re^{0.5} = 2 \left[ f''(0) - \left( \frac{\alpha_1}{3} \right) f'''(0) \right].$$

### 3.2 Heat transfer rate

The local Nusselt Number is defined as:

$$Nu = \frac{xq_w}{k(T_w - T_\infty)},$$

where,  $q_w$  symbolize surface heat flux and defined as:

$$q_w = \frac{k + 16\sigma^*T_\infty^3}{3k^*} \partial_y T \quad \text{at } y = 0,$$

Thus

$$Nu Re^{0.5} = -\left(\frac{1}{1 - n_1}\right) \left(1 + \frac{4}{3} Rd\right) \theta'(0).$$

### 3.3 Sherwood number

The local Sherwood Number is interpreted as:

$$Sh_x = \frac{xq_m}{D_B(\phi_w - \phi_\infty)},$$

where,  $q_m$  represents surface mass flux and defined as:

$$q_m = -D_B(\partial_y \phi) \quad \text{at } y = 0,$$

Thus

$$Sh_x Re^{0.5} = -\left(\frac{1}{1 - n_2}\right) \phi'(0).$$

### 3.4 Density number of micro-organisms distribution

The local density number of micro-organisms is defined as:

$$N_n = \frac{xq_i}{D_m(N_w - N_\infty)},$$

where,  $q_i$  characterize motile micro-organisms flux and defined as:

$$q_i = -D_m(N_y \phi) \quad \text{at } y = 0,$$

Thus

$$N_n Re^{0.5} = -\left(\frac{1}{1 - n_3}\right) \xi'(0).$$

## 4 Implementation of method

In this segment, the numerical result of resulting dimensionless nonlinearity coupled ordinary differential equations

Eq. (19) to Eq. (22) with boundary conditions Eq. (23) are integrated by MATLAB built-in raft (bvp4c). This computational software MATLAB is utilized for the substantiation of results of the shooting technique. To execute this numerical method, the differential equation Eq. (19-22) is transformed into a first-order ordinary differential equation by introducing some new notations and its implementation of some new variables expressed as below:

Let

$$f = y_1, f' = y_2, f'' = y_3, f''' = y_3', \theta = y_4, \theta' = y_5, \theta'' = y_5'$$

$$\phi = y_6, \phi' = y_7, \phi'' = y_7', \xi = y_8, \xi' = y_9, \xi'' = y_9'$$

$$y_3' = y_2^2 - y_1 y_3 + A\left(\frac{\eta}{2}\right) y_3 + y_2 - M(E_1 + y_2)$$

$$-\omega(y_4 - N r y_6 - N c y_8)$$

$$y_5' = \frac{-Pr[N b y_5 y_7 + N y_5^2 + Ec M(y_2 + E_1)^2 - 2 y_2 y_4 + y_1 y_5 + Ec(y_3)^2 - A\left(\frac{\eta}{2}\right) y_5 + 2 y_4]}{(1 + \left(\frac{4}{3}\right) Rd)}$$

$$y_7' = -\frac{Nt}{Nb} y_6' - LePr[-y_1 y_7 - y_2 y_6 - \sigma[1 + \delta y_4]^n$$

$$\exp\left[\frac{-E_a}{1 + \delta y_4}\right] - \gamma y_6 - A\left(\frac{\eta}{2}\right) y_7 + 2 y_6]$$

$$y_9' = -L b y_1 y_9 + 2 L b y_2 y_8 + A\left(\frac{\eta}{2}\right) y_9 + 2 y_8 - Pe[y_9 y_7$$

$$+ (\delta + y_8) y_7]$$

$$y_1 = R, y_2 = 1 + R_1 y_3, y_4 = 1, y_4' = -1, y_6 = 1 + R_2 y_7,$$

$$y_8 = 1 + R_3 y_9, \text{ at } \eta = 0$$

$$y_2 = 0, y_4 = 0, y_6 = 0, y_8 = 0 \text{ as } \eta \rightarrow \infty$$

## 5 Results and discussion

The analysis clearly shows the relationship of numerical results. It is clear from Table 1 and Table 2 that there are close agreements among the results for the parameters under discussion  $\delta$  and  $Pr$  individually. The purpose of the present section is to describe the effect of physical and numerical results. The above code is run for acceptable ranges of the controlling parameters. Findings are obtained for velocity  $f'(\eta)$ , temperature  $\theta(\eta)$ , nano-particle volume fraction  $\phi(\eta)$  and micro-organism distribution  $\xi(\eta)$ . The numerical scheme is validated.

The impacts of various physical parameters like magnetic parameter  $M$ , activation energy parameter  $E_1$ , mixed convection parameter  $\omega$ , buoyancy ratio parameter

**Table 1** Comparison of skin friction coefficient for various values of  $\delta$

$\delta$	Khan and Azam (2017)	Daniel et al. (2020)	Present results
0.0	1.00000	1.000000	1.000000
0.2	1.06801	1.068012	1.068011
0.4	1.13469	1.134685	1.134677
0.6	1.19912	1.199117	1.199115
0.8	1.26104	1.261040	1.261048
1.2	1.37772	1.377720	1.377723

**Table 2** Comparison of Nusselt number for various values of  $Pr$

$Pr$	Chen (1998)	Fatunmbi and Okoya (2020)	Seddeek and Salem (2005)	Present results
0.72	1.08853	1.08853	1.08852	1.08853
1.0	1.33334	1.33333	1.33333	1.33333
3.0	2.50972	2.50972	2.50972	2.50972
7.0	3.97150	3.97151	-	3.97151
10.0	4.79686	4.79687	4.9751	4.79682

$Nr$ , Rayleigh number  $Rb$ , unsteady parameter  $A$ , Eckert number  $Ec$ , Brownian motion parameter  $Nb$ , thermophoresis parameter  $Nt$ , Prandtl number  $Pr$ , radiation parameter  $Rd$ , electric field parameter  $E_a$ , chemical reaction  $\gamma$ , Lewis number  $Le$ , bioconvection Lewis number  $Lb$ , Peclet number  $Pe$ , microorganisms difference parameter  $\delta$  on physical quantities are noticed for both PST and PHF cases. The values of  $M = 0.1, h = 0.5, S_1 = S_2 = S_3 = A = \omega = Nr = Nc = \delta_1 = Lb = Pe = 0.1, E_1 = 0.01, Rd = Ec = 0.2, Pr = 0.733, Nb = Nt = \sigma = n$

$= 0.5, E_a = 0.3, \gamma = 1, Le = 5$  are fixed in computational procedure.

The influence of the magnetic field parameter on velocity  $f'(\eta)$  is demonstrated in Fig. 3a. A retarding trend is shown for velocity profile with the uplifting of magnetic parameter  $M$ . The basic reason for retardation is resistance to flow due to Lorentz force. Figure 3b discloses the effective outcomes when activation energy parameter  $E_1$  is applied on velocity distribution. The arising curve depicts that the velocity curve rises when the activation energy parameter is intensified. The effect of parameter  $\omega$  on velocity distribution is depicted in Fig. 4a. It is observed that  $\omega$  is responsible for increasing boundary layer distribution in the presence of PST and PHF cases. The experimental behavior of buoyancy ratio parameter  $Nr$  over velocity field distribution is plotted through Fig. 4b. The decreasing trend is observed when parameter  $Nr$  is uplifted. The upthrust effect becomes stronger with stronger buoyancy force. Figure 5a is presenting the effect of Rayleigh number  $Nc$  for velocity distribution. The stronger points of combined convection of natural and forced convection give downward grades executing over stretching sheet

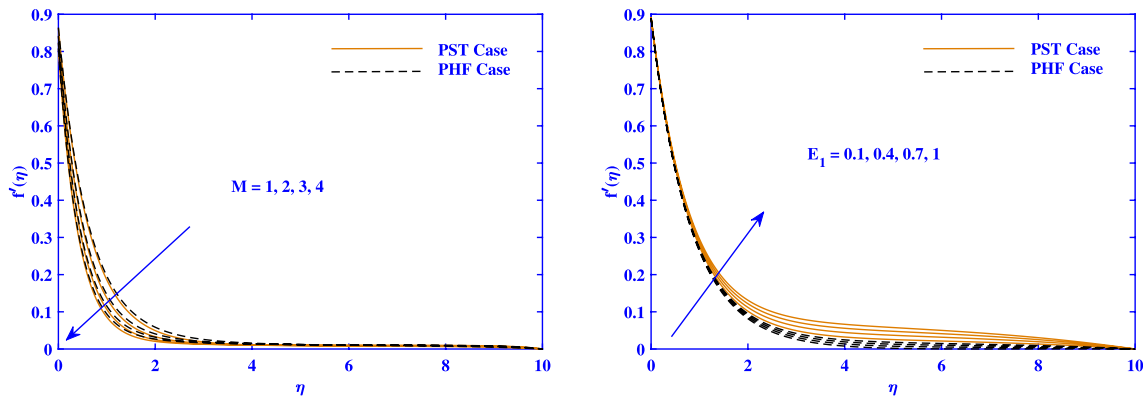


**Fig. 3** Fluctuation of  $f'(\eta)$  with  $M$  and  $E_1$

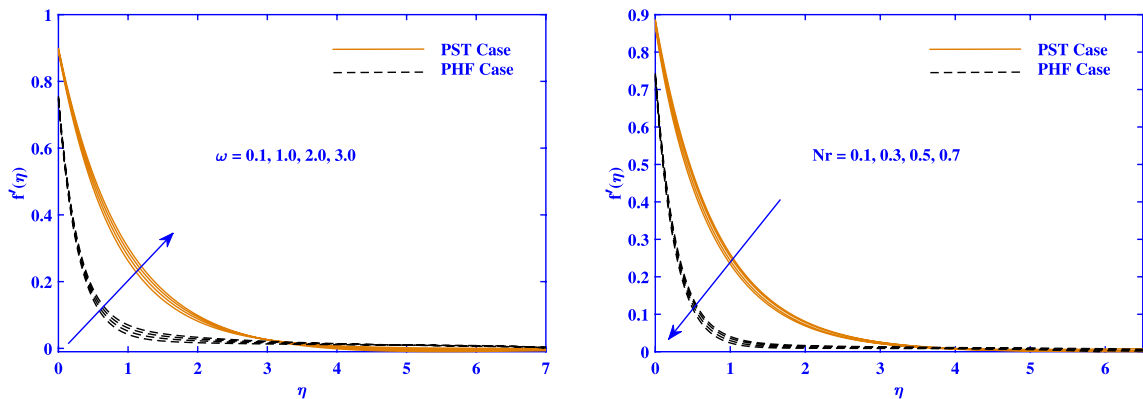


**Fig. 4** Fluctuation of  $f'(\eta)$  with  $\omega$  and  $Nr$



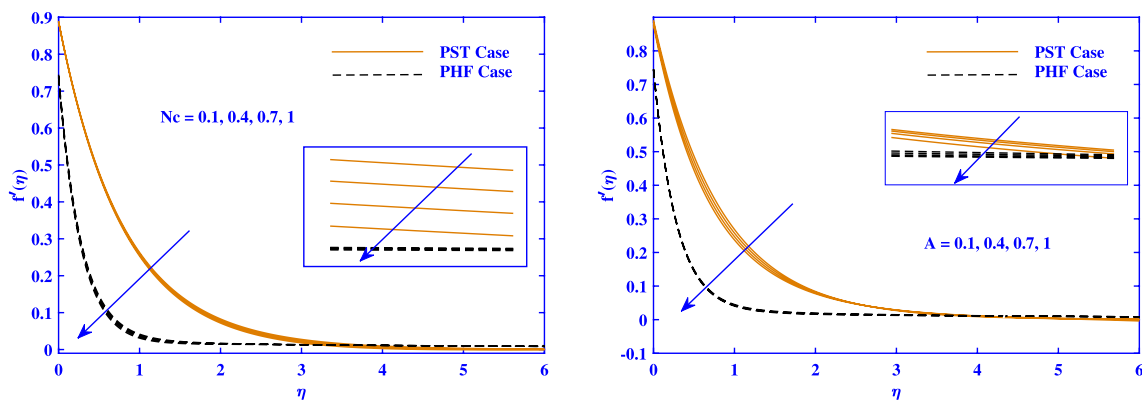


Fig. 5 Fluctuation of  $f'(\eta)$  with  $Nc$  and  $A$

for MHD Flow of unsteady flow. Figure 5b demonstrate the impact of unsteady parameter  $A$  on the velocity profile. It is seen from the figure that the velocity profile gets decreasing for both PST and PHF cases with the increasing values of  $A$ . Due to decreasing behavior of velocity profile, the thickness of momentum boundary also reduces. The magnetic effect over thermal distribution is sketched in Fig. 6a. The increasing values of magnetic parameter intensify the heat distribution along the stretching sheet for both PST and PHF cases. The influence of activation energy for temperature distribution is exhibited in Fig. 6b. It can be visualized that activation energy causes a decreasing effect of temperature coefficient on enlarging  $E_1$ . Another significant parameter that is used to characterize heat transfer dissipation is discussed along temperature coefficient is pictured through Fig. 7a. The outcomes revealed that temperature  $\theta(\eta)$  is intensified when the  $Ec$  parameter is increased. The temperature of the fluid is also when the mixed convection parameter  $\omega$  is intensified as shown in Fig. 7b. It is observed that when mixed convection parameter is uplifted, it reduces the temperature of nanofluid. On the other hand, Fig. 8 and

b illustrate the firmness between Brownian motion  $Nb$  and thermophoresis parameter  $Nt$  on both cases for PST and PHF. These two parameters show similar behavior on the increasing values of temperature. The impact of buoyancy ratio parameter  $Nr$  on thermal boundary layer distribution is described in Fig. 9a. Plots describe that when buoyancy ratio has uplifted the nanofluid comprising MHD flow have a larger amount of temperature  $\theta(\eta)$ . Figure 9b illustrates the effect of Prandtl number  $Pr$  over-temperature distribution. The findings show that increasing  $Pr$  decreases the temperature of nanofluid. The effect of radiation parameter  $Rd$  over temperature is discussed in Fig. 10a. The input effects came to conclude that large values of the  $Rd$  parameter take to a higher amount of temperature coefficient. Figure 10b shows the behavior of unsteady parameter  $A$  on temperature distribution for PST and PSH. It is observed that with the rising values of unsteady parameter  $A$ , the temperature decreases monotonically. The impact of unsteady parameter  $A$  is seen more projecting for temperature than the velocity profile. Figure 11a presents the influence of parameter  $\sigma$  on concentration profile. Increasing the amount of  $\sigma$  causes to

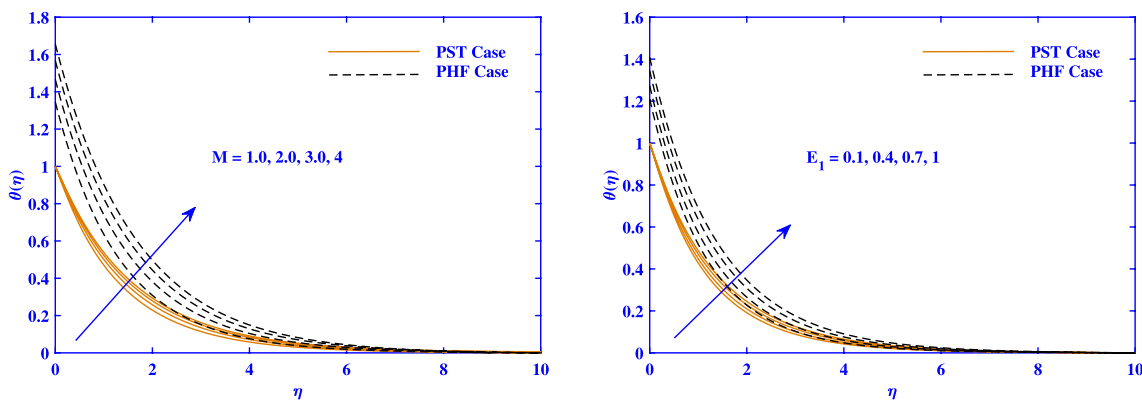


Fig. 6 Fluctuation of  $\theta(\eta)$  with  $M$  and  $E_1$

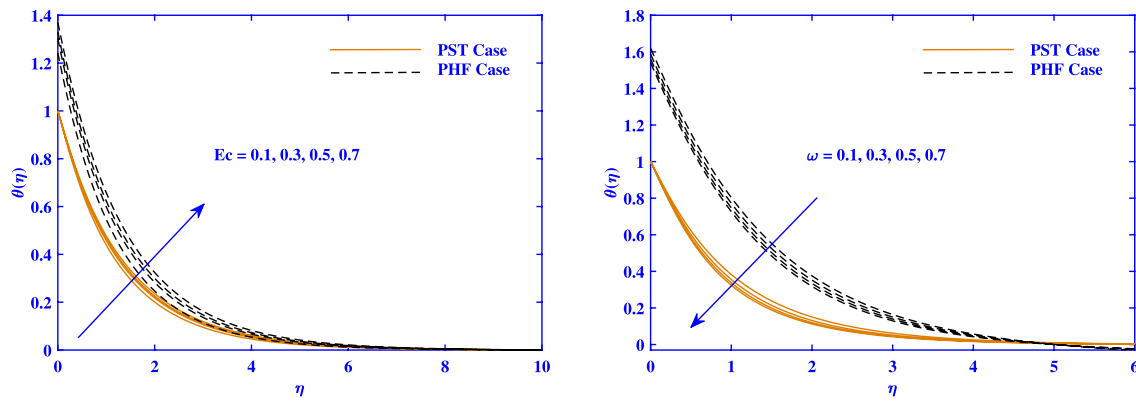


Fig. 7 Fluctuation of  $\theta(\eta)$  with  $Ec$  and  $\omega$

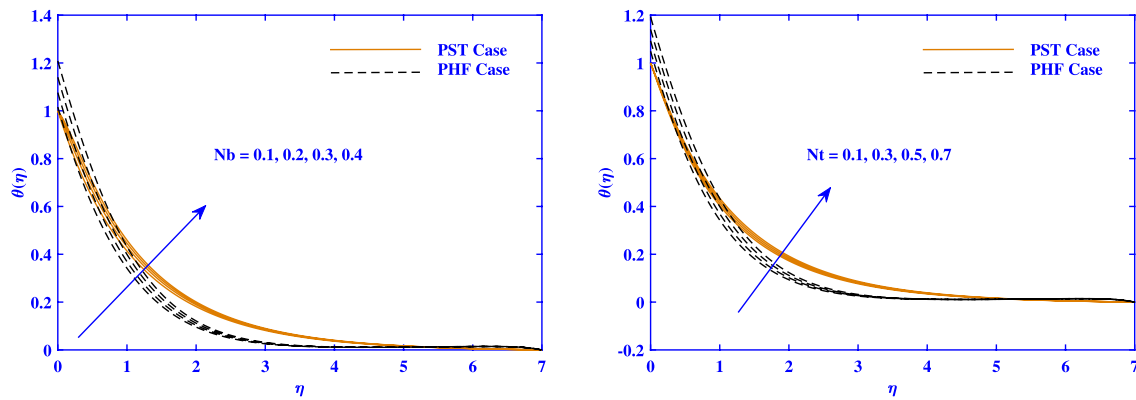


Fig. 8 Fluctuation of  $\theta(\eta)$  with  $Nb$  and  $Nt$

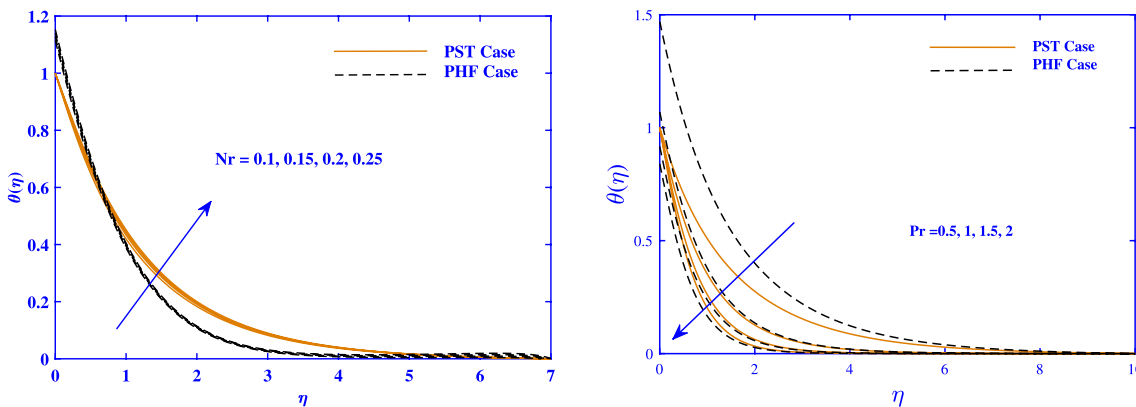


Fig. 9 Fluctuation of  $\theta(\eta)$  with  $Nr$  and  $Pr$

decrease in concentration profile. The opposite behavior for activation energy parameter  $E_a$  is shown in Fig. 11b. A significant parameter affecting the concentration profile while the execution of MHD flow of unsteady nanofluid is the chemical reaction parameter  $\gamma$ . The physical results depict

that the concentration profile is reduced when  $\gamma$  is intensified. The result report can be visualized in Fig. 12a. Figure 12b shows that the nanoparticle concentration decreases as the fitted rate constant  $n$  increases. The physical behavior for concentration profile for a significant parameter i.e.

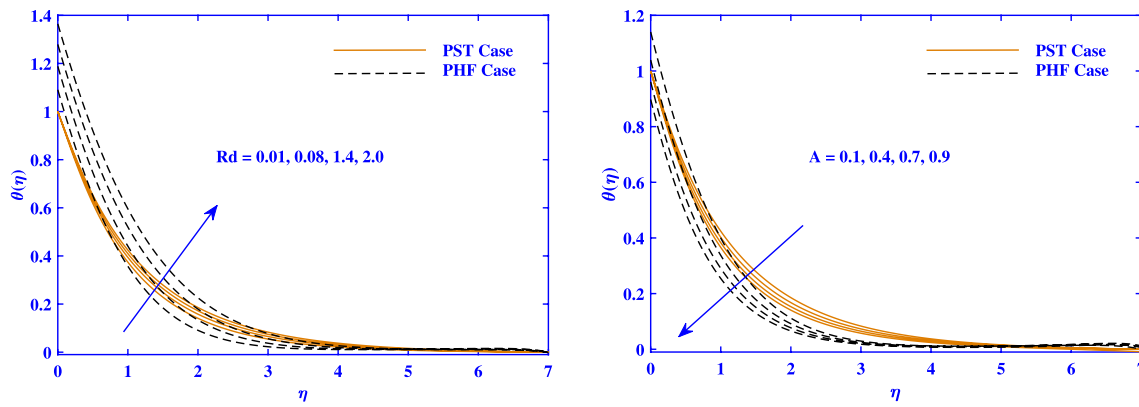


Fig. 10 Fluctuation of  $\theta(\eta)$  with  $Rd$  and  $A$

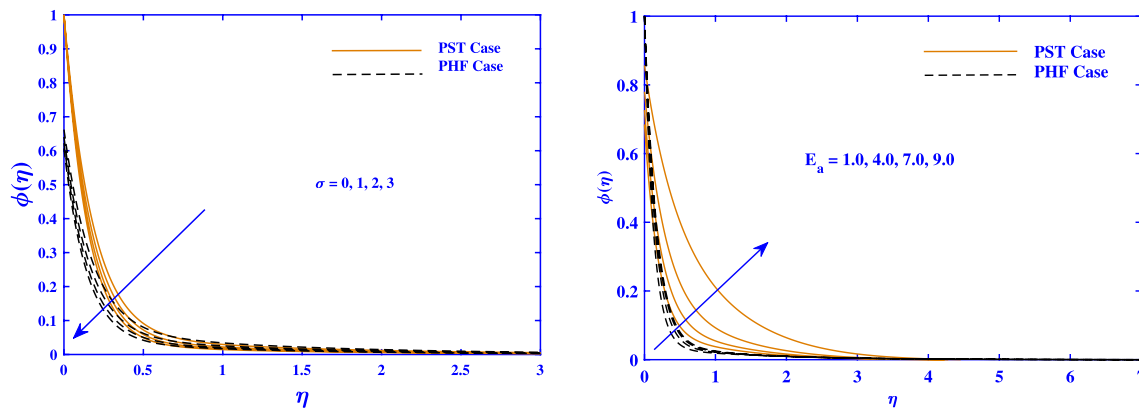


Fig. 11 Fluctuation of  $\phi(\eta)$  with  $\sigma$  and  $E_a$

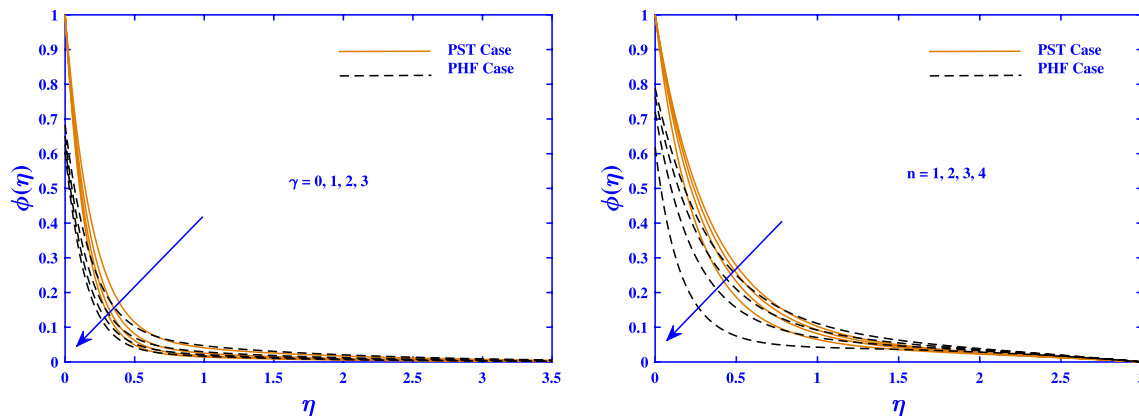


Fig. 12 Fluctuation of  $\phi(\eta)$  with  $\gamma$  and  $n$

Brownian motion is sketched by Fig. 13a. Observing the trends shows that the concentration profile decreases down while uplifting the  $Nb$  parameter. To disclose the physical behavior of thermophoresis parameter over concentration distribution for MHD flow of nanofluid Fig. 13b is drawn.

It is brought to conclude that the rising  $Nt$  parameter leads to an increment in concentration distribution. As  $Nt$  is the phenomenon of the combined effect of moving particles of the fluid in which different forces of temperature gradient are the reason of increment in concentration field. Observing the

effect of Lewis number  $Le$  with respect to the concentration profile, it is seen that  $\phi(\eta)$  is reduced. The evidence report of the above conclusion is reported in Fig. 14a. The physical impact of unsteady parameter  $A$  over the concentration field

is displayed in Fig. 14 (b). Unsteady parameter produces a decreasing curve for the concentration distribution. Figure 15a is the illustration of bioconvection Lewis number  $Lb$  and its effect upon motile microorganism distribution.

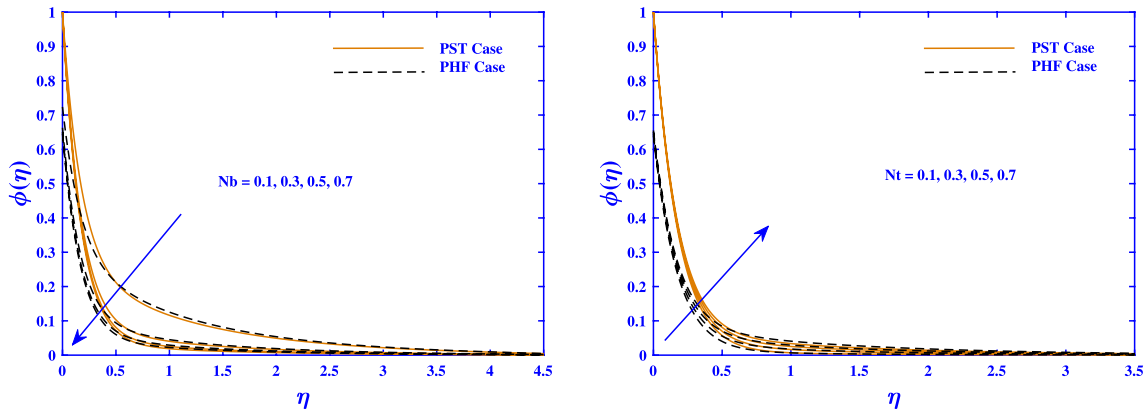


Fig. 13 Fluctuation of  $\phi(\eta)$  with  $Nb$  and  $Nt$

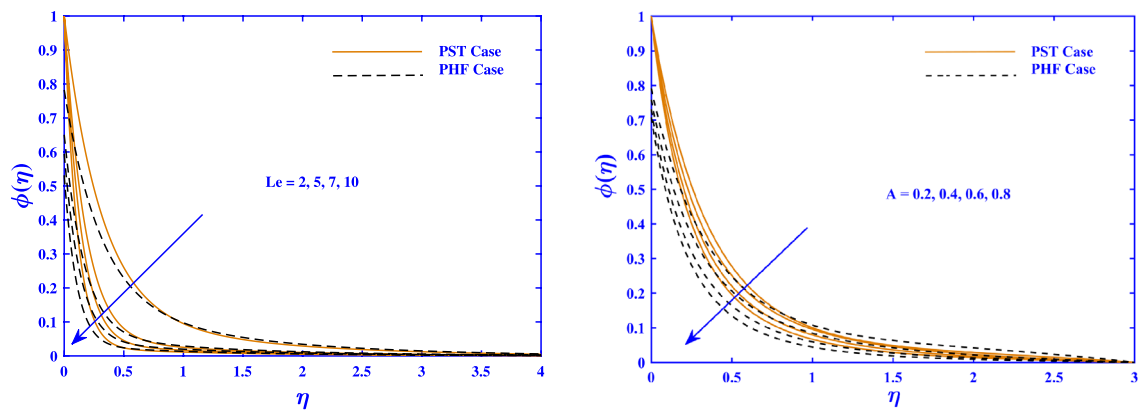


Fig. 14 Fluctuation of  $\phi(\eta)$  with  $Le$  and  $A$

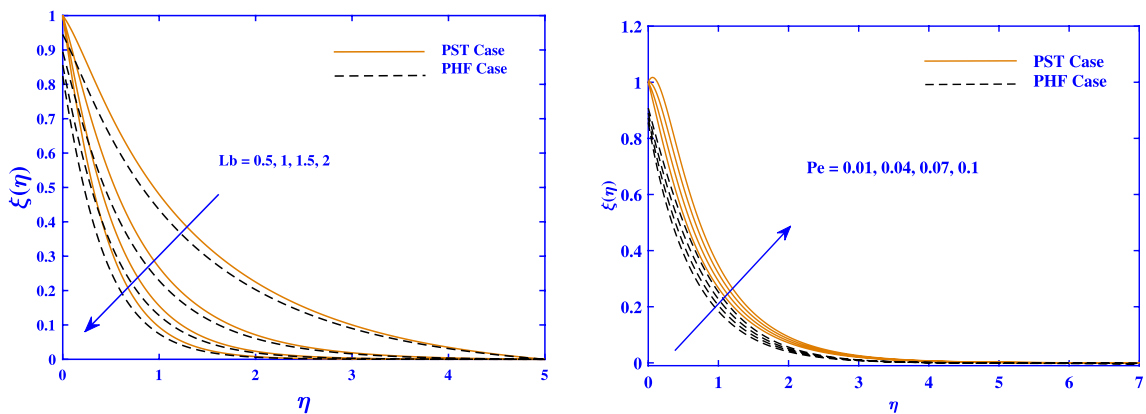
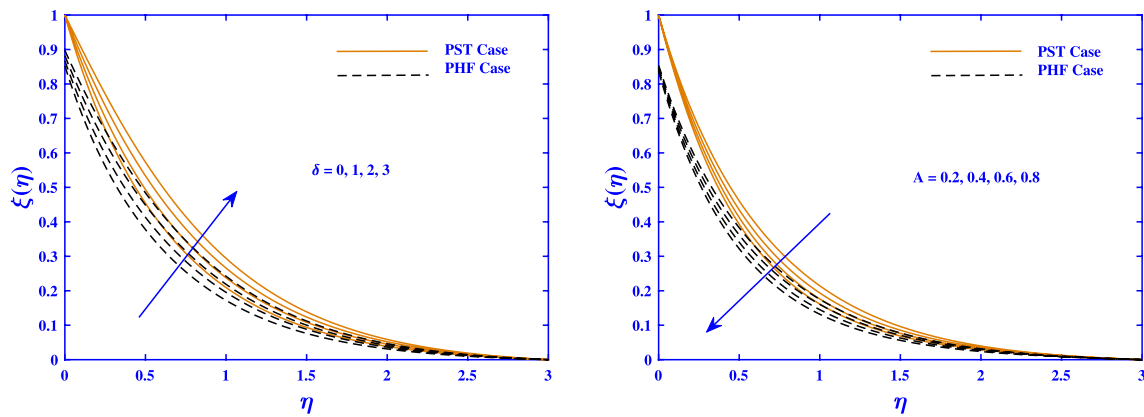


Fig. 15 Fluctuation of  $\xi(\eta)$  with  $Lb$  and  $Pe$



**Fig. 16** Fluctuation of  $\xi(\eta)$  with  $\delta$  and  $A$

The traces reveal that motility of the nanofluid decreases when the  $Lb$  parameter is raised. The physical effect of Peclet number  $Pe$  and motile microorganism distribution is deployed in Fig. 15b. Motility profile is observed rising in curves as Peclet number is given larger amount. Microorganisms difference parameter is a significant parameter affecting the motility of nanofluid having MHD flow. An increase is observed when  $\delta$  is intensified as depicted in Fig. 16a. The impact of an unsteady parameter over motile microorganism distribution is discussed in Fig. 16b. It is visualized that when a large amount of unsteady parameter is given as an input, it gives a rising curve of motile microorganism profile.

## 6 Conclusions

An investigation for bioconvection and radiative effects for MHD time-dependent flow of nanofluids due to an extending domain is made theoretically and numerically. Velocity, temperature, concentration, and motile microorganisms' profiles are evaluated for two types of thermal conditions namely, PST and PHF with varying inputs of pertinent parameters. The requirement of efficient heat transfer is managed by nanoparticle diffusion with enhancement of thermal conductivity of crude base fluid. The bioconvection of self motile microorganisms can be useful to avoid undesired sedimentation. The findings of this communication can find applications in heat exchangers, microelectronics and cooling of nuclear reactors.

- Velocity trends are enhanced for higher mixed while it shows a decrement for magnetic and buoyancy ration parameter in the presence of the electric field.
- Concentration is uplifted for a larger amount of Biot number while reduction is observed for Brownian motion.

- The motility of the nanofluids shows declination for greater values of Peclet number and bioconvection Lewis number.
- Thermalboundary layer distribution is decreased when Prandtl number under the cases of slip (PST) and (PHF).
- The concentration of nanoparticles increased for a larger solutal Biot number.
- The microorganism concentration reduces for various variations of Peclet number and bio convection Lewis number.
- The current model refers to an enhanced approach to the thermal conductivity of the base fluid and used in nano-technology.

## References

- Abbasi F, Shanakhat I, Shehzad S, Hamida MBB (2021) Squeezed flow of water-based nanofluid having temperature dependent viscosity and thermal conductivity. *Phys Scr* 96(6):065214
- Abdal S, Hussain S, Ahmad F, Ali B (2015) Hydromagnetic stagnation point flow of micropolar fluids due to a porous stretching surface with radiation and viscous dissipation effects. *Sci Int* 27:3965–3971
- Abdal S, Ali B, Younas S, Ali L, Mariam A (2020) Thermo-diffusion and multislip effects on mhd mixed convection unsteady flow of micropolar nanofluid over a shrinking/stretching sheet with radiation in the presence of heat source. *Symmetry* 12(1):49
- Abdal S, Hussain S, Siddique I, Ahmadian A, Ferrara M (2021a) On solution existence of mhd casson nanofluid transportation across an extending cylinder through porous media and evaluation of priori bounds. *Sci Rep* 11(1):1–16
- Abdal S, Siddique I, Afzal S, Chu Y-M, Ahmadian A, Salahshour S (2021b) On development of heat transportation through bioconvection of maxwell nanofluid flow due to an extendable sheet with radiative heat flux and prescribed surface temperature and prescribed heat flux conditions. *Math Methods Appl Sci*. <https://doi.org/10.1002/mma.7722>
- Abdal S, Alhumade H, Siddique I, Alam MM, Ahmad I, Hussain S (2021c) Radiation and multiple slip effects on

- magneto-hydrodynamic bioconvection flow of micropolar based nanofluid over a stretching surface. *Appl Sci* 11(11):5136
- Abdal S, Mariam A, Ali B, Younas S, Ali L, Habib D (2021d) Implications of bioconvection and activation energy on reiner-rivlin nanofluid transportation over a disk in rotation with partial slip. *Chin J Phys* 73:672–683
- Adshead P, Holder G, Ralegankar P (2020) Bbn constraints on dark radiation isocurvature. *J Cosmol Astropart Phys* 9:016
- Ahmad F, Abdal S, Ayed H, Hussain S, Salim S, Almatroud A (2021) The improved thermal efficiency of maxwell hybrid nanofluid comprising of graphene oxide plus silver/kerosene oil over stretching sheet. *Case Stud Therm Eng* 27:101257
- Ahmed Z, Nadeem S, Saleem S, Ellahi R (2019) Numerical study of unsteady flow and heat transfer cnt-based mhd nanofluid with variable viscosity over a permeable shrinking surface. *Int J Numer Meth Heat Fluid Flow* 29(12):4607–4623
- Alamri SZ, Khan AA, Azeez M, Ellahi R (2019) Effects of mass transfer on mhd second grade fluid towards stretching cylinder: a novel perspective of cattaneo-christov heat flux model. *Phys Lett A* 383(2–3):276–281
- Alblawi A, Malik MY, Nadeem S, Abbas N (2019) Buongiorno's nanofluid model over a curved exponentially stretching surface. *Processes* 7(10):665
- Ali L, Liu X, Ali B, Mujeed S, Abdal S (2019) Finite element simulation of multi-slip effects on unsteady mhd bioconvective micropolar nanofluid flow over a sheet with solutal and thermal convective boundary conditions. *Coatings* 9(12):842
- Ali L, Liu X, Ali B, Mujeed S, Abdal S, Mutahir A (2020a) The impact of nanoparticles due to applied magnetic dipole in micropolar fluid flow using the finite element method. *Symmetry* 12(4):520
- Ali L, Liu X, Ali B, Mujeed S, Abdal S, Khan SA (2020b) Analysis of magnetic properties of nano-particles due to a magnetic dipole in micropolar fluid flow over a stretching sheet. *Coatings* 10(2):170
- Ali B, Abdal S, Shafiq A, Siddique I (2021) Magneto-hydrodynamic mass and heat transport over a stretching sheet in a rotating nanofluid with binary chemical reaction, non-fourier heat flux, and swimming microorganisms. *Case Stud Therm Eng* 28:101367
- Almheiri A, Hartman T, Maldacena J, Shaghoulia E, Tajdini A (2020) Replica wormholes and the entropy of hawking radiation. *J High Energy Phys* 2020:13
- Bassett BR, Owen JM, Brunner TA (2020) Efficient smoothed particle radiation hydrodynamics II: radiation hydrodynamics. *J Comput Phys* 429(9):109994
- Bazdar H, Toghraie D, Pourfatah F, Akbari OA, Nguyen HM, Asadi A (2020) Numerical investigation of turbulent flow and heat transfer of nanofluid inside a wavy microchannel with different wavelengths. *J Therm Anal Calorim* 139(3):2365–2380
- Bhatti M, Michaelides EE (2020) Study of Arrhenius activation energy on the thermo-bioconvection nanofluid flow over a riga plate. *J Therm Anal Calorim* 143:2029–2038
- Buongiorno J (2006) Convective transport in nanofluids. *J Heat Transfer* 128(3):240–250
- Chen C-H (1998) Laminar mixed convection adjacent to vertical, continuously stretching sheets. *Heat Mass Transf* 33(5–6):471–476
- Choi SU, Eastman JA (1995) Enhancing thermal conductivity of fluids with nanoparticles. Tech. rep., Argonne National Lab., IL (United States)
- Daniel YS, Aziz ZA, Ismail Z, Salah F (2017) Entropy analysis of unsteady magneto-hydrodynamic nanofluid over stretching sheet with electric field. *Int J Multiscale Comput Eng* 15(6):545–565
- Daniel YS, Aziz ZA, Ismail Z, Bahar A, Salah F (2020) Slip role for unsteady mhd mixed convection of nanofluid over stretching sheet with thermal radiation and electric field. *Indian J Phys* 94(2):195–207
- Eid MR, Mahny K, Dar A, Muhammad T (2020) Numerical study for carreau nanofluid flow over a convectively heated nonlinear stretching surface with chemically reactive species. *Physica A* 540:123063
- Ellahi R, Sait SM, Shehzad N, Mobin N (2019a) Numerical simulation and mathematical modeling of electro-osmotic couette-poiseuille flow of mhd power-law nanofluid with entropy generation. *Symmetry* 11(8):1038
- Ellahi R, Zeeshan A, Hussain F, Abbas T (2019b) Thermally charged mhd bi-phase flow coatings with non-newtonian nanofluid and hafnium particles along slippery walls. *Coatings* 9(5):300
- Fatunmbi EO, Okoya SS (2020) Heat transfer in boundary layer magneto-micropolar fluids with temperature-dependent material properties over a stretching sheet. *Adv Mater Sci Eng* 5:5. <https://doi.org/10.1155/2020/5734979>
- Gonçalves HM, Neves SA, de Zea Duarte A, Bermudez V (2020) Nanofluid based on carbon dots functionalized with ionic liquids for energy applications. *Energies* 13(3):649
- Gorniy V, Salman A, Tronin A, Shilin B (1988) Terrestrial outgoing infrared radiation as an indicator of seismic activity. *Proc Acad Sci USSR* 301(1):67–69
- Habib D, Abdal S, Ali R, Baleanu D, Siddique I (2021) On bioconvection and mass transpiration of micropolar nanofluid dynamics due to an extending surface in existence of thermal radiations. *Case Stud Therm Eng* 27:101239
- Habib D, Salamat N, Abdal S, Siddique I, Ang MC, Ahmadian A (2022) On the role of bioconvection and activation energy for time dependent nanofluid slip transpiration due to extending domain in the presence of electric and magnetic fields. *Ain Shams Eng J* 13(1):101519
- Hamid A, Khan MI, Kumar RN, Gowda RP, Prasannakumara B (2021) Numerical study of bio-convection flow of magneto-cross nanofluid containing gyrotactic microorganisms with effective prandtl number approach. *Sci Rep* 11:16030
- He W, Toghraie D, Lotfipour A, Pourfatah F, Karimipour A, Afrand M (2020) Effect of twisted-tape inserts and nanofluid on flow field and heat transfer characteristics in a tube. *Int Commun Heat Mass Transfer* 110:104440
- Ibrahim W, Shankar B (2013) Mhd boundary layer flow and heat transfer of a nanofluid past a permeable stretching sheet with velocity, thermal and solutal slip boundary conditions. *Comput Fluids* 75:1–10
- Jilte R, Kumar R, Ahmadi MH (2019) Cooling performance of nanofluid submerged vs nanofluid circulated battery thermal management systems. *J Clean Prod* 240:118131
- Khan M, Azam M (2017) Unsteady heat and mass transfer mechanisms in mhd carreau nanofluid flow. *J Mol Liq* 225:554–562
- Khan SA, Nie Y, Ali B (2019) Multiple slip effects on magneto-hydrodynamic axisymmetric buoyant nanofluid flow above a stretching sheet with radiation and chemical reaction. *Symmetry* 11(9):1171
- Mabood F, Rauf A, Prasannakumara B, Izadi M, Shehzad S (2021) Impacts of stefan blowing and mass convection on flow of maxwell nanofluid of variable thermal conductivity about a rotating disk. *Chin J Phys* 71:260–272
- Mir S, Akbari OA, Toghraie D, Sheikhzadeh G, Marzban A, Mir S, Talebizadehsardari P (2020) A comprehensive study of two-phase flow and heat transfer of water/ag nanofluid in an elliptical curved minichannel. *Chin J Chem Eng* 28(2):383–402
- Nasiri H, Jamalabadi MYA, Sadeghi R, Safaei MR, Nguyen TK, Shadloo MS (2019) A smoothed particle hydrodynamics approach for numerical simulation of nano-fluid flows. *J Therm Anal Calorim* 135(3):1733–1741
- Noghrehabadi A, Izadpanahi E, Ghalambaz M (2014) Analyze of fluid flow and heat transfer of nanofluids over a stretching sheet near the extrusion slit. *Comput Fluids* 100:227–236
- Punith Gowda R, Naveen Kumar R, Jyothi A, Prasannakumara B, Nisar KS (2021a) Kkl correlation for simulation of nanofluid flow over

- a stretching sheet considering magnetic dipole and chemical reaction. *ZAMM J Appl Math* 101:e202000372
- Punith Gowda RJ, Naveen Kumar R, Jyothi AM, Prasannakumara BC, Sarris IE (2021b) Impact of binary chemical reaction and activation energy on heat and mass transfer of Marangoni driven boundary layer flow of a non-Newtonian nanofluid. *Processes* 9(4):702
- Ramesh G, Roopa G, Rauf A, Shehzad S, Abbasi F (2021) Time-dependent squeezing flow of casson-micropolar nanofluid with injection/suction and slip effects. *Int Commun Heat Mass Transf* 126:105470
- Rauf A, Abbas Z, Shehzad SA (2019a) Magnetohydrodynamics slip flow of a nanofluid through an oscillatory disk under porous medium supremacy. *Heat Transf-Asian Res* 48(8):3446–3465
- Rauf A, Abbas Z, Shehzad S (2019b) Interactions of active and passive control of nanoparticles on radiative magnetohydrodynamics flow of nanofluid over oscillatory rotating disk in porous medium. *J Nanofluids* 8(7):1385–1396
- Saqib M, Ali F, Khan I, Sheikh NA, Shafie SB (2019) Convection in ethylene glycol-based molybdenum disulfide nanofluid. *J Therm Anal Calorim* 135(1):523–532
- Sarada K, Gowda RJP, Sarris IE, Kumar RN, Prasannakumara BC (2021) Effect of magnetohydrodynamics on heat transfer behaviour of a non-newtonian fluid flow over a stretching sheet under local thermal non-equilibrium condition. *Fluids* 6(8):264
- Seddeek M, Salem A (2005) Laminar mixed convection adjacent to vertical continuously stretching sheets with variable viscosity and variable thermal diffusivity. *Heat Mass Transf* 41(12):1048–1055
- Shah Z, Khan A, Khan W, Alam MK, Islam S, Kumam P, Thounthong P (2020) Micropolar gold blood nanofluid flow and radiative heat transfer between permeable channels. *Comput Methods Programs Biomed* 186:105197
- Shi Q-H, Hamid A, Khan MI, Kumar RN, Gowda R, Prasannakumara B, Shah NA, Khan SU, Chung JD (2021) Numerical study of bio-convection flow of magneto-cross nanofluid containing gyrotactic microorganisms with activation energy. *Sci Rep* 11(1):1–15
- Srinivasacharya D, Sreenath I (2020) Unsteady bioconvection in a squeezing flow of a couple-stress fluid through horizontal channel. *Int J Appl Comput Math* 6(2):1–16
- Yahya AU, Salamat N, Huang W-H, Siddique I, Abdal S, Hussain S (2021) Thermal characteristics for the flow of williamson hybrid nanofluid (mos2+ zno) based with engine oil over a stretched sheet. *Case Stud Therm Eng* 26:101196
- Yahya AU, Salamat N, Habib D, Ali B, Hussain S, Abdal S (2021) Implication of bio-convection and cattaneo-christov heat flux on williamson sutterby nanofluid transportation caused by a stretching surface with convective boundary. *Chin J Phys* 73:706–718
- Yusuf TA, Mabood F, Prasannakumara B, Sarris IE (2021) Magneto-bioconvection flow of Williamson nanofluid over an inclined plate with gyrotactic microorganisms and entropy generation. *Fluids* 6(3):109

**Publisher's Note** Springer Nature remains neutral with regard to jurisdictional claims in published maps and institutional affiliations.